Philosophical Magazine
Publication details, including instructions for authors and subscription information:
http://www.tandfonline.com/loi/tphm20

Realistic nano-polycrystalline microstructures: beyond the classical Voronoi tessellation

Alberto Leonardi [a], Paolo Scardi [a] & Matteo Leoni [a]
[a] Department of Materials Engineering and Industrial Technologies, University of Trento, Trento, Italy

Version of record first published: 06 Jan 2012

To cite this article: Alberto Leonardi, Paolo Scardi & Matteo Leoni (2012): Realistic nano-polycrystalline microstructures: beyond the classical Voronoi tessellation, Philosophical Magazine, 92:8, 986-1005

To link to this article: http://dx.doi.org/10.1080/14786435.2011.637984

Philosophical Magazine
Vol. 92, No. 8, 11 March 2012, 986–1005

Taylor & Francis
Taylor & Francis Group

Realistic nano-polycrystalline microstructures: beyond the classical Voronoi tessellation

Alberto Leonardi, Paolo Scardi and Matteo Leoni*

Department of Materials Engineering and Industrial Technologies, University of Trento, Trento, Italy

(*Received 7 February 2011; final version received 26 October 2011*)

A modified Voronoi tessellation (MVT) is proposed for the computer simulation of realistic microstructures. Compared with standard tessellations, the present algorithm provides the desired grain size distribution in a one-step, non-evolutionary procedure. This is obtained by relaxing the constraints of Voronoi tessellation on position and orientation of the grain boundaries, with the only side effect being the formation of a limited amount of eliminable voids. As an example, it is shown how to directly obtain a distribution of grains of given variance and with a shape statistically close to the lognormal one.

Keywords: nanograined structure; microstructure; molecular dynamics; Voronoi tessellation; grain size distribution

1. Introduction

Atomistic modelling is increasingly employed for the study and prediction of the properties of materials at the nano scale. The starting point of all these studies is a realistic model for the microstructure [1–3], including grain shape and size distribution, chemical composition, atomic positions, as well as specific models of grain boundaries. The microstructure, in fact, plays a key role in determining the mechanical and physical properties of a polycrystalline aggregate [4–7]: poor microstructure modelling might lead to results that, albeit correct, are not representative of a real object [8]. Statistical properties are especially relevant: grain arrangement, shape and size distributions, as typically observed by a transmission electron microscope, have usually a peculiar behaviour that is far from being random [9] and thus needs to be accurately reproduced.

To simulate a microstructure, a net of connected closed cells should be created. The operation, also known as space tessellation, is not trivial. Several algorithms have been proposed for periodic [10], aperiodic [11–13] and for stochastic tessellation: Delaunay triangulation (DT [14,15]), Voronoi tessellation (VT [16–21]), Laguerre tessellation (LT [22,23]) and Johnson–Mehl tessellation (JMT [24,25]) are traditionally employed to create interconnected cells with no gaps [3]. The starting point for all tessellations is a box, in most cases with imposed periodic boundary conditions

*Corresponding author. Email: Matteo.Leoni@unitn.it

ISSN 1478–6435 print/ISSN 1478–6443 online

http://dx.doi.org/10.1080/14786435.2011.637984
http://www.tandfonline.com

(PBCs), in which a set of points (centres or generators) is laid. The point creation process and the algorithm generating the associated cells differentiate the various tessellation methods. A homogeneous Poisson point process with parameter λ is a convenient and commonly adopted generator, as it is compatible with the study of aggregates obtained from random nucleation sites [19,20,26].

Voronoi tessellation (VT) is the most popular in several fields of research [27–29] owing to its simplicity [30–33], space-filling nature and to the availability of theoretical results on the topological properties (especially in the case of Poisson–Voronoi tessellation (PVT)) [19,20,26,34–40]. Although VT leads to microstructures closely resembling real ones, topological and statistical properties (e.g. dihedral angles, number of triple junctions, area of grain boundaries and junction lengths) are not always compatible with experimental results [41]. For instance, in a PVT the cell volumes follow a distribution close to a gamma distribution [6,18], certainly not the most common in the literature on materials analysis where the lognormal distribution prevails [1–2,6,42–45]. To obtain grains with a different distribution, the available options are to employ a different point process (e.g. Ginibre–Voronoi [33] or Laguerre–Voronoi [46–48] tessellations), or to start with a traditional VT and to modify the positions of the generators using an evolutionary approach, e.g. constrained Voronoi tessellation (CVT) [8,41] or the method of Suzudo and Kaburaki [49].

Neither the traditional tessellation algorithms, nor these alternative methods, however, are able to directly produce an ensemble of cells with a lognormal distribution of volumes of arbitrary variance. The CVT has in principle the flexibility to do that for distributions narrower than the PVT, but always with tedious extra computing and at the expenses of the grain shape that becomes arbitrary.

In this paper we propose a new method, the modified Voronoi tessellation (MVT), that eliminates most limitations of traditional tessellations and provides a network of cells with a given size distribution, albeit at the expenses of leaving some eliminable small voids. To be fully correct, the result is therefore a pattern and not a tessellation. It will be also shown that a distribution of domains possessing a target variance and a shape statistically close to the lognormal can be obtained directly from a random distribution of centres, without the need for extra evolutionary steps. The topological properties of the obtained ensemble will be presented and compared with the existing literature.

2. Modified Voronoi tessellation (MVT)

Voronoi tessellation enforces a dependence of the cell shape on the mutual positioning of the generators: this limits and constrains the possible configurations and topological properties that can be obtained when describing the packed arrangements of objects with a given distribution. To better clarify this point and its implications, let's consider the simple case of a cluster of randomly arranged spheres (effectively mimicking an aggregate of equiaxed grains) with a lognormal distribution of diameters (see Figure 1a). Clearly, the Voronoi tessellation obtained from the centres of the spheres does not match the actual microstructure (see the dashed lines and the shaded area in Figure 1a). Voronoi tessellation is in fact unable to randomly

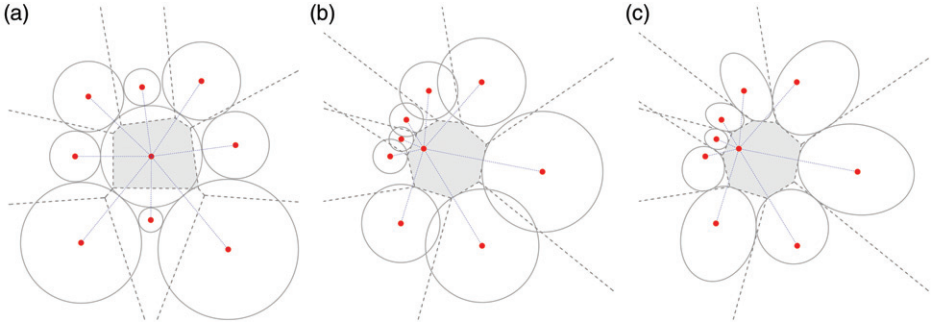

Figure 1. (a) Random packing of spheres with a lognormal distribution of diameters. The centres of the spheres form the dashed Voronoi net. (b) Trying to pack spherical objects around a given (quasi-)spherical one (grey). The Voronoi points needed to create the grey object must be centres of intersecting spheres. (c) To avoid intersections, the neighbouring objects have to be deformed.

pack a given set of unequal spheres: once a (quasi-)spherical shape of the cells is chosen and a given sphere is selected (grey cell in Figure 1b), the possible size and position of the neighbouring cells is determined. Given a point, the direction where to place a neighbour determines the orientation of a face of the cell (direction and face are orthogonal), whereas the distance fixes the cell size along that direction. To avoid the unphysical resulting superposition (cf. Figure 1b), the neighbouring objects should then elongate (Figure 1c). This is an intrinsic limitation of Voronoi tessellation that goes beyond the sophisticate evolutionary procedures employed e.g. by Gross and Li [8] and by Suzudo and Kaburaki [49] to build a microstructure with a given distribution. The impossibility of VT to pack equiaxed objects is also the main reason why any evolutionary method inevitably creates non-spherical cell shapes (see Figure 1c).

As a matter of fact, any tessellation based on the classical norm (excluding the JMT) would lead, in a real case, to polyhedral grains approximating the spheres and not to true spheres. The microstructure of Figure 1a is actually compatible with a Laguerre tessellation with generators in the centres of the spheres; to obtain a Laguerre tessellation of a given sphere set, first a random close packing of spheres (RCPS) must be calculated [47]. This computationally-intensive step cannot be avoided and is not easily parallelisable.

To quickly and directly reproduce an arrangement like the one depicted in Figure 1a starting from randomly positioned centres, we propose a modified Voronoi tessellation (MVT). The main differences between PVT (but also VT in general) and MVT lays in the configuration of the cell–cell interface. In particular, its position along the distance of neighbouring centres (plane interface position, PIP) and its orientation with respect to the plane orthogonal to that vector (plane interface orientation, PIO) are modified. Changing these factors, i.e. going towards a more realistic nucleation/growth process (as in the LT and JMT methods), allows the simulation of realistic microstructures with various statistical distributions of geometrical properties and grain types.

The release of position and orientation of the plane interface is obtained by introducing two additional factors in the geometric procedure of the VT

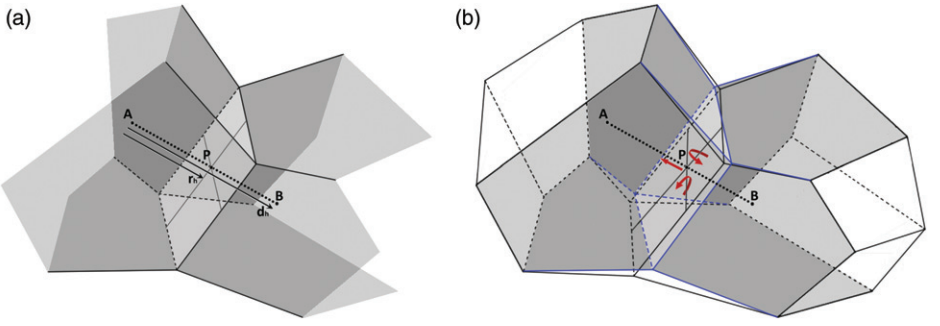

Figure 2. Neighbouring grains. (a) Traditional Voronoi tessellation. Poisson–Voronoi generators A and B and corresponding Voronoi PIP (P). The distance between the generators d_{AB} and the distance of the PIP from A (r_A) are also shown. (b) Modified Voronoi tessellation. The three possible operations introduced by the modified method, i.e. shift and two rotations of the plane interface.

(cf. Figure 2): a growth factor (GF) displacing each PIP from the mid-point between two generators and a rotation factor (RF) that changes the associated PIO. The growth factor is obtained as the product of a cell growth factor (CGF) isotropic for the cell, plus a face growth factor (FGF) taking into account a directional dependence of the cell expansion (or contraction). The PIP along the segment connecting two nearest centres A and B is obtained by equilibrating the GF of the corresponding grains, as in:

$$\begin{aligned} &GF_A = CGF_A \cdot FGF_{AB}, \quad GF_B = CGF_B \cdot FGF_{BA}, \\ &PIP = d_{AB} GF_A/(GF_A + GF_B), \end{aligned} \tag{1}$$

where d_{AB} is the distance between A and B.

To allow for PIOs not permitted by the Voronoi tessellation, the rotation factors (or better the rotation angles (ψ, θ) along two normal axes centred on the Voronoi PIP) are introduced. Clearly, the VT is obtained from MVT assuming constant GF and null RFs.

The analogies between MVT and VT suggest the possibility to apply an evolutionary procedure (that can be seen as a combination of those proposed in [8,49]) to further refine the resulting microstructure and to virtually obtain any predetermined statistical property for the aggregate. This constrained modified Voronoi tessellation (CMVT) will be presented elsewhere [50].

The cells in MVT are convex polyhedra, but they are usually not space filling: some void regions are created at the cell junctions, as the relaxation of the Voronoi tessellation constraints does not guarantee the compatibility of the geometry of the cells. These voids can be seen as a closed porosity and can form connected networks so counting them has a limited meaning. The presence of the voids is not a serious limitation for the aim of the present work, i.e. the application of the MVT to build a microstructure. Independently of the porosity, the boundary microstructures obtained by filling the cells with atoms are non-physical and need at least a MD equilibration [41,51]. Therefore, as there is no definitive experimental result on the

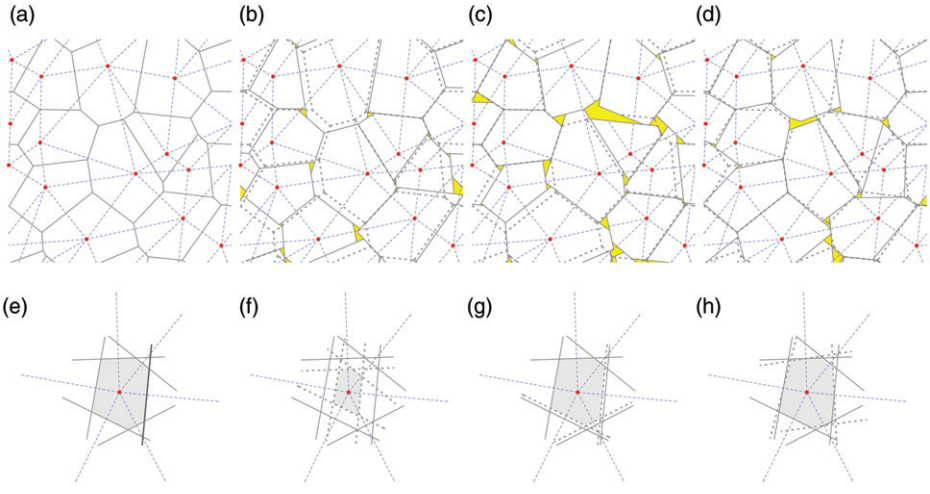

Figure 3. Changes in the microstructure caused by a different choice of model parameters. (a) Voronoi construction. (b) MVT with a lognormal distribution of CGF, $\mu = 1$, $\sigma = 0.30$. (c) MVT with different FGF (100 for $\langle 1\ 0\ 0 \rangle$, 75 for $\langle 1\ 1\ 1 \rangle$ and 50 for $\langle 0\ 1\ 1 \rangle$). (d) MVT with random perturbation of the PIO (limited to $\pm 20^\circ$). In (e), (f), (g) and (h), the detailed construction of a cell with the conditions (a), (b), (c) and (d), respectively. The dashed lines show the modifications occurring to the Voronoi cell in the various cases.

boundary structure [52], several methods can be proposed to take the voids into account or to eliminate them when filling the cells with atoms: some alternatives will be proposed in next section.

As shown in the following, a certain deterministic nature exists in the MVT, thus allowing for a direct linking of input parameters and statistical properties of the resulting simulated models.

3. MVT simulations: results and discussion

3.1. *Atomic density and voids in MVT-derived microstructures*

To visually compare the effects induced by different point growth factors on the resulting microstructure, a pseudo-planar case was simulated. A set of centres was produced using a Poisson process with $\lambda = 1$ on a square planar region with periodic boundary conditions. Starting from the same set of 14 points, four different microstructures were generated using different MVT setups (see Figure 3). In Figure 3a, the classical PVT is shown: the interfaces are halfway between neighbouring points and space filling is guaranteed. In Figure 3b a lognormal distribution of CGF described as:

$$f(x) = \frac{1}{x\sigma\sqrt{2\pi}} \exp\left(-\left(\frac{\ln x - \mu}{2\sigma} \right)^2 \right) \tag{2}$$

with $\sigma = 0.30$, $\mu = 1.00$ was chosen. The shape and size of the domains modifies and a fraction of empty volume is generated in the impingement points of three or more

grains. The quantity and the extension of the void regions can be changed by using a more complex set of parameters: in Figure 3c for instance three different FGF (100 for ⟨1 0 0⟩, 75 for ⟨1 1 1⟩ and 50 for ⟨0 1 1⟩; directions referred to the orientation of the local crystallographic reference chosen for each cell) are selected, whereas in Figure 3d a random perturbation of the interface angles (in the $\pm 20.0^{\circ}$ range) is applied.

The incoherent positioning of the interfaces is the cause for the presence of voids in the MVT: this results in a larger flexibility, as a large spread in atomic density can be obtained by suitably choosing the modelling parameters and by careful filling of the voids. Coherent modifications in the position of the interfaces would have resulted in space filling, but at the expenses of MVT generality.

Voids are filled when the atoms are placed inside the pattern of cells. Four alternatives are here proposed (Figure 4):

(1) leaving voids empty (Figure 4a): this would effectively simulate a packed aggregate of grains as obtained, e.g. in a packed powder;
(2) filling voids with a glass phase of given density (Figure 4b). This would allow a system with completely incoherent grain boundaries to be simulated;
(3) filling voids with additional grains possessing independent orientation (Figure 4c). A fully crystalline structure is obtained, but a possibly unphysical large fraction of very small grains is introduced in the system;
(4) growing neighbouring grains into the voids (Figure 4d). Slightly irregular grain shapes are obtained, but maximum density can be reached. The process is similar to the Johnson–Mehl growing but here a more complex picture of CGF and FGF can be taken into account.

The maximum quantity of atoms that can be placed in the box is not fixed, but depends on factors such as:

- the method used to fill in the cells with the crystallographic structure (for example, a realistic microstructure can be obtained by deleting atoms closer than 85% of the first neighbours distance [41]);
- the way the pattern of cells is built, and the statistical properties of the microstructure (size distribution, grains number and shape type).

However, independently of all other parameters, the number of grains (i.e. centres) is the key factor to determine the relative atomic density (AD, defined

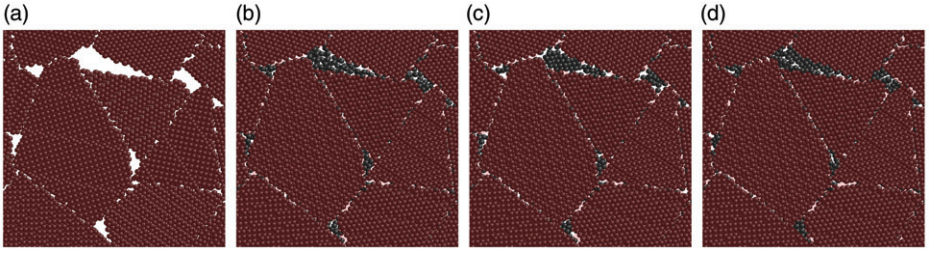

Figure 4. Filling of the void resulting from the MVT with (a) empty space (no filling), (b) amorphous phase, (c) crystalline phase and (d) extension of the grains. See text for details.

as the ratio between the actual atomic density and the maximum one) for a cluster (cf. Figure 5a). Due to the presence of voids, the atomic density obtained with the MVT is intrinsically lower than that given by the PVT; the difference disappears when the voids are filled using the fourth model (see list above, cf. Figure 5a).

Increasing the number of centres N causes a decreases of the atomic density and a corresponding increase in the surface-area-to-volume ratio (SA/V): the two curves in Figure 5a can be well reproduced by the two exponentials $\mathrm{AD} = 0.92455 + 0.05106\exp(N/290.938)$ and $\mathrm{SA}/V = 0.14626 - 0.1669\exp(-N/306.434)$.

Even for a single grain, full atomic density is never obtained in the general case unless box and lattice are suitably chosen (e.g. box scaled with respect to the unit cell and box corners sitting on lattice points).

In any case, nanomaterials cannot be simulated with full atomic density owing to the presence of a large fraction of lower-density grain boundaries where empty volume accumulates. The situation presented in Figure 5a, however, refers only to the geometrical construction: changes are expected when the geometrical microstructure is evolved using, e.g. molecular statics or molecular dynamics.

The actual values of the input parameters of MVT have a strong effect on the space filling ability. A decrease in space filling ability is usually observed when increasing the dispersion of growth and rotation factors: however, the trend is not monotonous and it is possible to find combinations of parameters which give a better filling of the space. The relative space filling (SF, fraction of volume occupied by the cells in a unity volume inside the box) is independent of the density of centres in the simulation box and decreases steadily for increasing breadth of the input distribution. As an example, Figure 5b shows the case of a lognormal distribution of CGF with $\mu = 1$. The curve can be well modelled as $\mathrm{SF} = 1 - 0.01449\sigma - 0.069477\sigma^2$. When increasing the breadth of the input distribution of CGFs, the distribution of the SF becomes more symmetrical (the skewness approaches zero) and its standard deviation becomes proportionally larger (see Figure 5b). It is clear that the higher the σ (i.e. the wider the distribution of sizes), the more difficult is to get a random spatial arrangement of the objects, thus the higher the chances that empty regions (voids) remain (lower space fill). An increase in space filling with respect to Figure 5b can be obtained by using the CMVT method [50].

3.2. *Statistical properties of the MVT*

It is quite interesting to study further the microstructures obtained by MVT when imposing a lognormal distribution of CGF, all other modification parameters being zero (i.e. GF equal to CGF). Figure 6a shows the average cell volume (V) distributions for the microstructures resulting from the application of the MVT method to the same set of 5000 centres using different lognormal distributions of CGF. The specimens will be identified as MVT x L y, where x is the number of centres and y is the σ of the lognormal distribution of CGF ($\mu = 1.0$). Lognormal curve fits are also provided in Figure 6a as a guide for the eye. For a given distribution of CGF, the result does not modify if the CGF associated to each centre, the μ of the CGF and the box dimensions are changed.

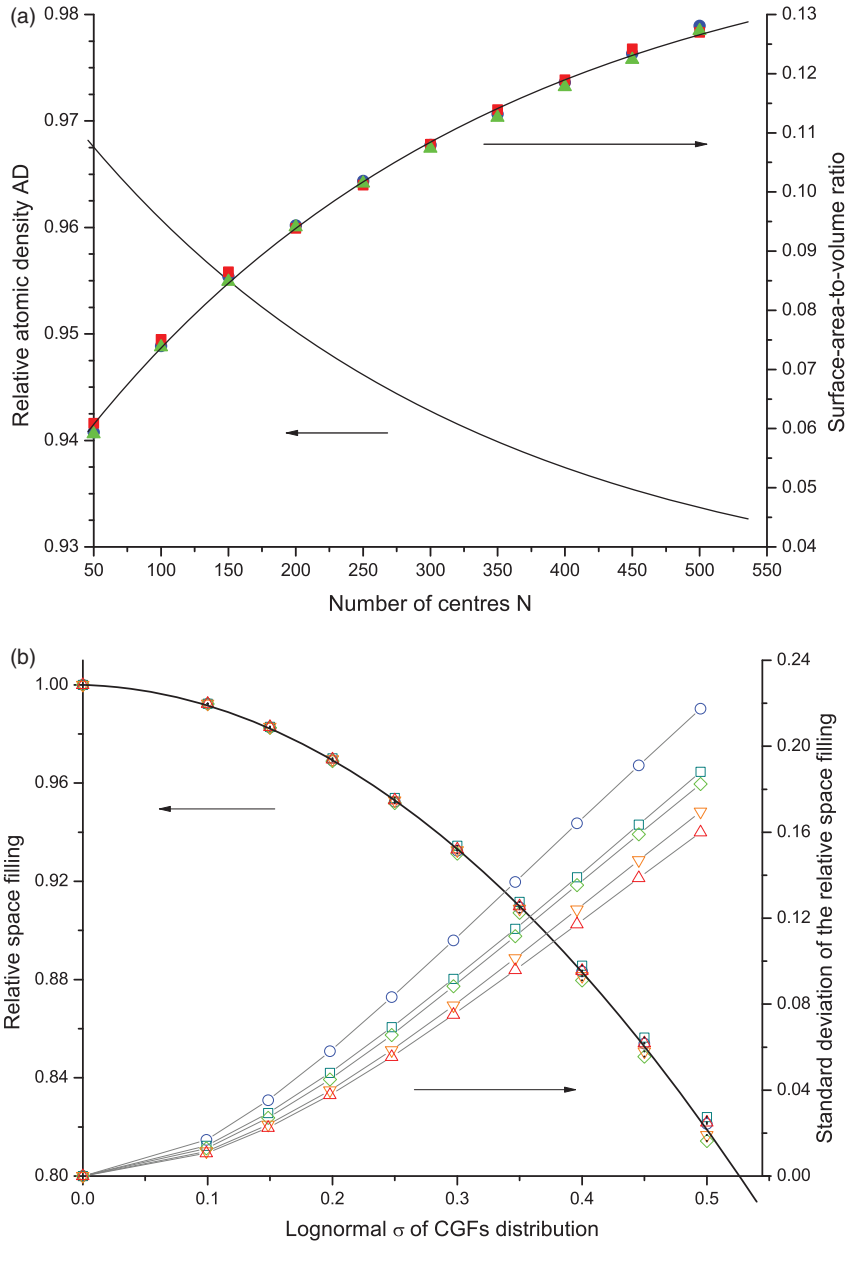

Figure 5. (Colour online). (a) Relative atomic density and surface-area-to-volume ratio versus number of centres for four pattern methods: (i) PVT (circle), (ii) CVT with target lognormal distribution $\sigma = 0.15$ (square), (iii) MVT with a lognormal distribution of CGF having $\sigma = 0.10$ (diamond) and (iv) same as (iii) but with voids filled according to model F4 (triangle). (b) Statistical properties (mean and standard deviation) of the relative space filling in the model versus lognormal σ for the MVT as a function of the number of centres: 1000 (circle), 2000 (square), 3000 (diamond), 4000 (down triangle) and 5000 (up triangle).

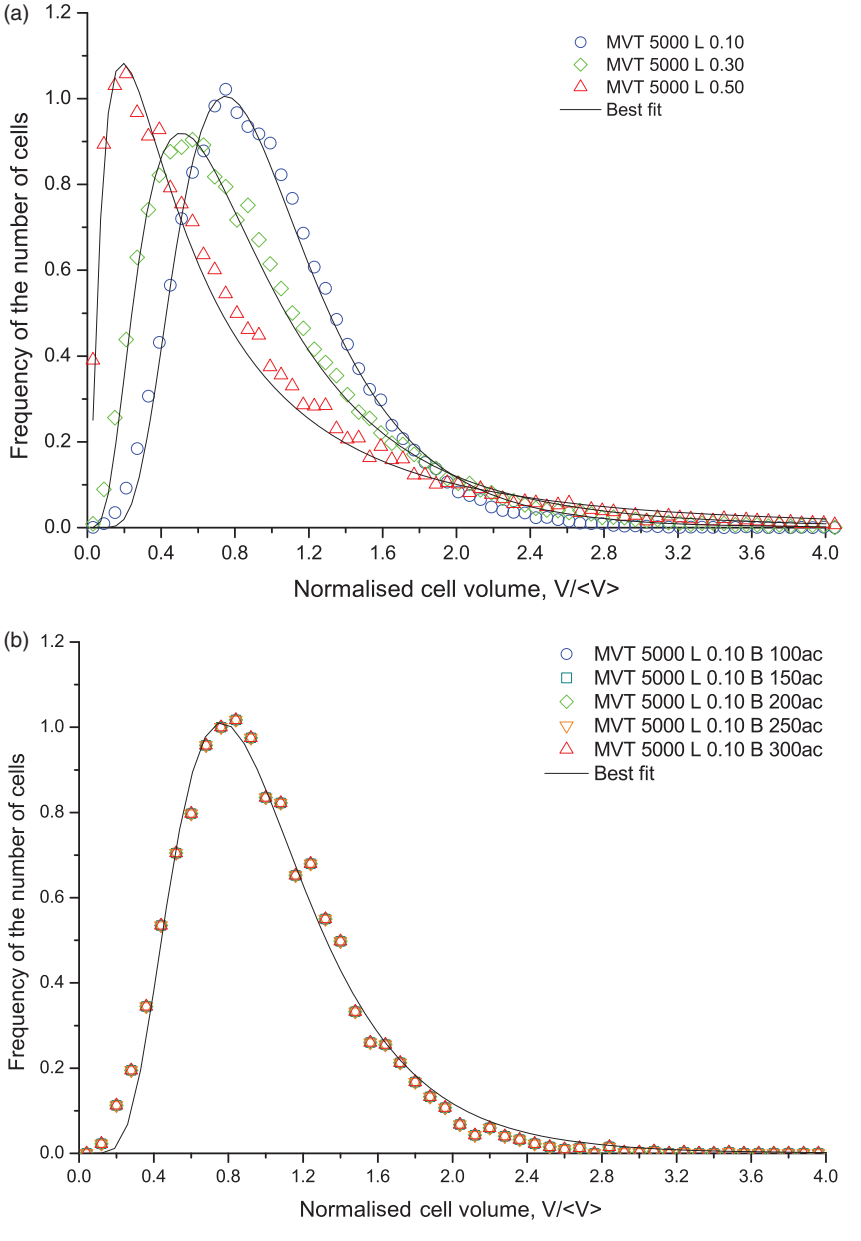

Figure 6. (Colour online). Cell volume distribution for a few MVT 5000 samples obtained (a) with different CGF distributions and (b) with fixed distribution ($\sigma = 0.1$) and increasing box size expressed as number of unit cells along the edge: 100 (circle), 150 (square), 200 (diamond), 250 (up triangle), 300 (down triangle). In (c) and (d), respectively, the distributions of total cell surface area and number of faces per cell. The curve proposed by Tanemura [56] is shown in (d) as continuous line.

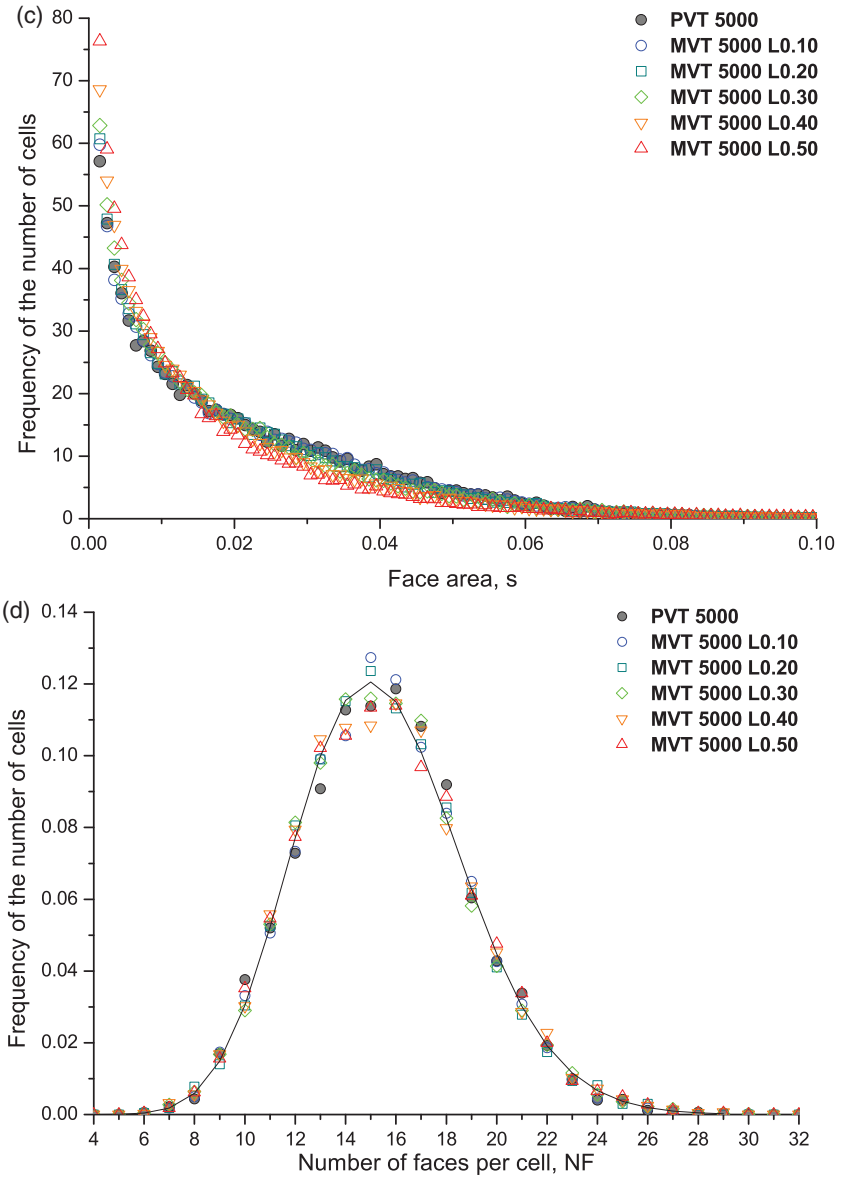

Figure 6. (Colour online). Continued.

The cell volume is just a possible parameter to characterise the size of irregular objects such as the tessellation cells. The equivalent volume cell radius, total cell surface area, face surface area and number of faces per cell (NF), are also employed to characterise the topology of the resulting objects. It can be observed that the distributions of cell radius and cell surface area obtained with a lognormal distribution of CGF are close to lognormal too. The cumulative distribution functions (CDFs) were compared in the case of some samples made by several

number of centres (1000 to 5000) and lognormal variances of the CGFs ($\sigma = 0.10$ to 0.50). The largest difference between the observed and the best fitted lognormal CDFs are below the 5% critical Kolmogorov–Smirnov limit. Moreover, the smaller the number of centres and the variance of the lognormal distribution of the CGFs, the higher is the level of significance. For instance, significance is larger than 10% in the case of MVT 1000 samples. The mean of the resulting distribution depends on box size and number of points, i.e. on the average volume per point, whereas the variance depends only on the input parameters and is unaffected by the box size. This is clearly shown in Figure 6b, which shows analysis of some MVT 5000 samples made with the same lognormal distribution of CGFs ($\mu = 1.0$ and $\sigma = 0.10$) but increasing box size. The independence on box size of the statistical properties allows a coherent scaling of the results obtained on a sample to any other one.

As expected (Figure 6c), the surface area of the faces and their frequency are almost inversely related. Quite different is the behaviour of NF shown in Figure 6d: all simulated microstructures show exactly the same distribution whose mean (15.5352) is very close to the average facedness of the PVT ($2 + 48\pi^2/35 \approx 15.53547$ [26,53,54]) and whose shape is compatible with the slightly-skewed generalised gamma distribution proposed by Tanemura [54]. The agreement comes from the fact that the mutual arrangement of the centres and thus the average number of near neighbours, is not changed by the MVT.

The number of faces is sufficient to characterise several topological properties of the cell. In fact, by using Euler's formula for convex polyhedra we can relate NF with the number of vertices (NV) and the number of edges (NE) of a cell as NV – NE + NF = 2. The NV can in turn be computed using the equation: NV = 2NF – 4. The changes in NF and in the average volume of the corresponding cell are usually linearly correlated through Lewis' law [55]: $\langle V \rangle_{NF} = \alpha_L(NF - NF_0)$. In the present case, however, a parabolic trend is evident (cf. Figure 7a): a parabolic violation of Lewis' law has been already pointed out in both simulated and measured dispersed polycrystalline microstructures [46,41,56–58].

The nonlinear trend seems associated to the process employed to lay the centres in the box. In fact, limiting the minimum distance between centres eliminates the nonlinearity: Figure 7b, for instance, shows the modification occurring to Figure 7a on increasing to 20 Å the minimum distance between generators. Small deviations from the trends occur at the edges of the NF curve owing to the limited statistics (number of grains) associated to those points. The parameters of the curves slightly change with the increase in the standard deviation of the cell volume distributions, but invariably intercept the axis at NF = 3 (degenerate case). This suggests that the deviation in the slopes of the MVT models is due to the presence of voids, decreasing the cell volume especially of the larger cells. The influence of the voids decreases with the cell size and the axis intercept agree with the impossibility to define a closed polyhedron with less than four faces.

A final check for the properties of the cell ensemble is provided by the ratio between the average number of faces in all neighbouring cells to a cell of NF faces (m(NF)) and the number of faces per cell. The relationship is well described by the Aboav–Weaire law [59]:

$$\mathrm{NF}m(\mathrm{NF}) = \mathrm{NF}[\langle \mathrm{NF} \rangle - \alpha] + [\langle \mathrm{NF} \rangle \alpha + \mu_2], \tag{3}$$

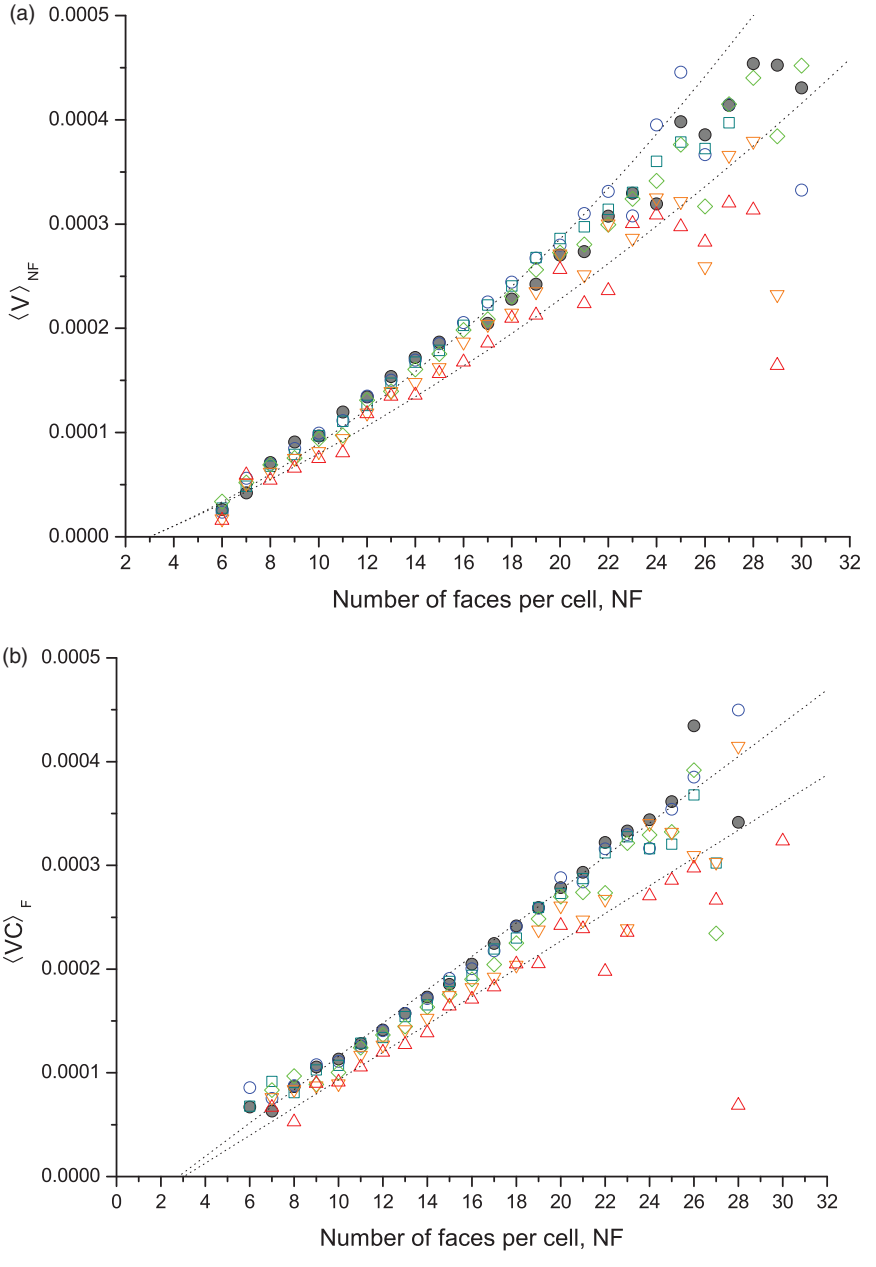

Figure 7. (Colour online). (a, b) Lewis plots for the MVT 5000 samples of Figure 6a. The plot in (b) was obtained by limiting the minimum distance between centres to 20 Å. In (c) the Aboav–Weaire plot is shown for the MVT 5000 samples of Figure 6a. Fits are proposed for the limiting cases MVT5000 L 0.1 and MVT 5000 L 0.5.

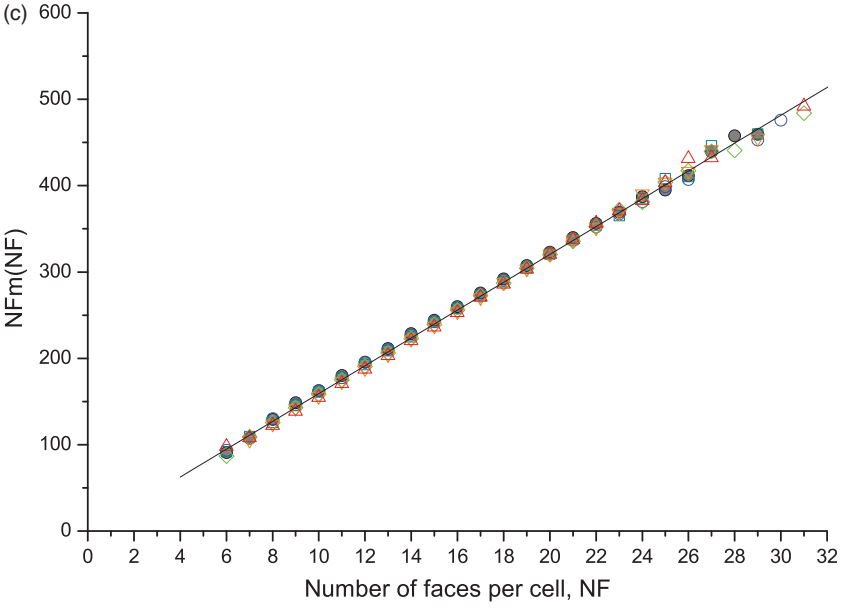

Figure 7. (Colour online). Continued.

where α and μ_2 are fitting parameters. Mathematically, this expresses the tendency for any random tessellation to have small grains surrounded by large ones and vice versa.

Plots for the cases analysed here are shown in Figure 7c: the MVT and PVT methods show exactly the same slope and the same deviation from the best linear fit. Different distributions, resulting from the PVT and MVT with lognormal CGF, lead to analogous trends: this is consistent with the fact that both algorithms start with a similar random arrangement of points and that the MVT does not heavily modify the number of faces of Voronoi cells (cf. Figure 6). A small downward curvature in Figure 7c seems to be present, confirming the observation of Hilhorst [53], thus strengthening the idea that the Aboav-Weaire law might be just a good local approximation for the correct trend. In the range shown, the modified curve proposed in [53], i.e. $\mathrm{NF}m(\mathrm{NF}) = 8\mathrm{NF} + 23.15\mathrm{NF}^{5/6} - 15.96\mathrm{NF}^{2/3}$ does not appreciably depart from Equation (3).

3.3. *Relationship between input parameters and resulting microstructure*

A systematic relationship exists between the input CGF distribution and the resulting cell size distribution. It should be stressed that different choices can lead to completely different resulting distributions. For the sake of brevity, just the lognormal case is analysed in detail. Without losing in generality, a collection of samples was simulated with increasing number of centres and different lognormal CGF distributions with lognormal mean $\mu = 1$. A cubic box with PBCs and a side

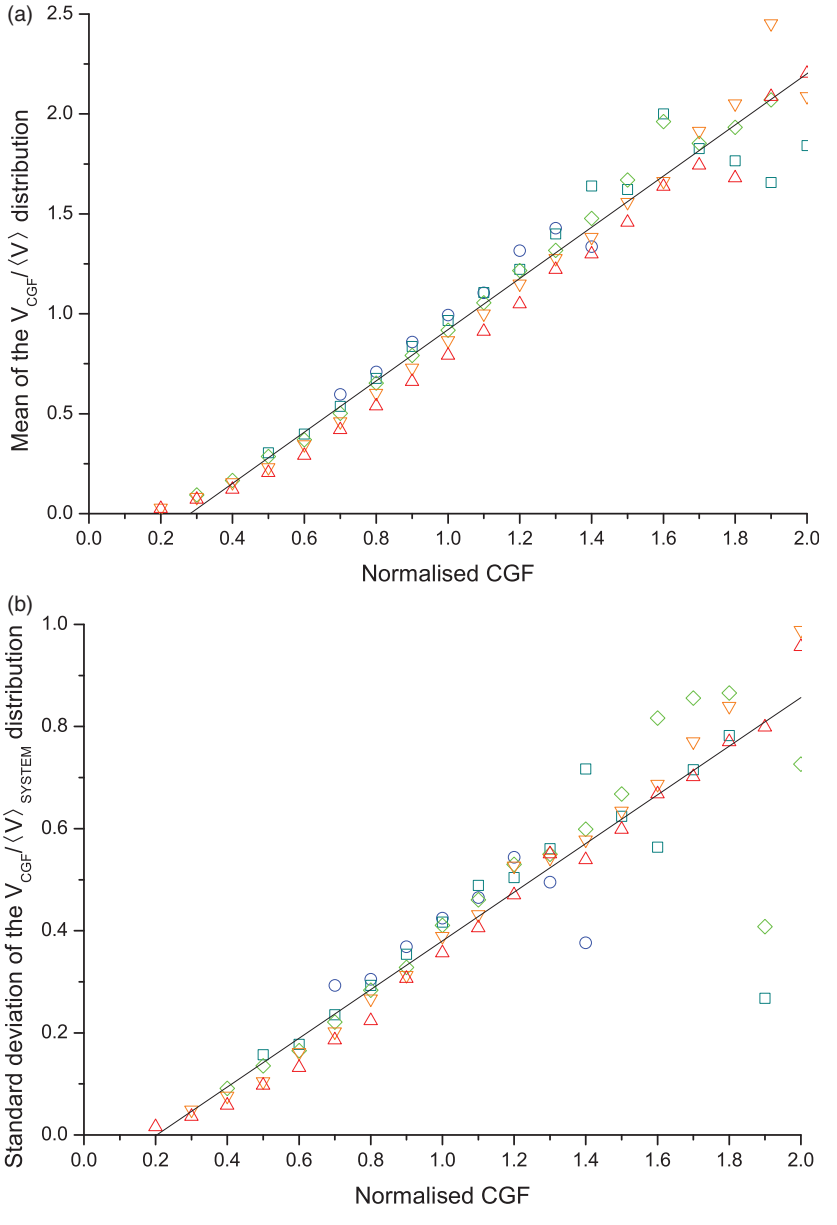

Figure 8. (Colour online). Mean (a) and standard deviation (b) of the normalised cell volume distributions as a function of the normalised CGF (where V_{CGF} is the volume of the cells having a reference CGF). Data relative to the MVT5000 L 0.10 (circle), MVT5000 L 0.20 (square), MVT5000 L 0.3 (diamond), MVT5000 L 0.4 (down triangle) and MVT5000 L 0.50 (up triangle).

of 100 unit cells was employed. The same naming convention for the samples proposed before will be used here.

As an example, Figure 8 shows the relationship between the input CGF and the corresponding mean and standard deviation of the (lognormal) grain volume

distribution. The direct dependence between CGF and mean cell volume (or size in general) expresses the fact that if the centres would be isolated, their size at a given time would be proportional to their growth rate. The standard deviation for each CGF value, on the other hand, is related to the magnitude of the difference between isolated growth and actual growth (constrained by the interference with the other centres). Therefore, the growth rate represents somehow the probability of interference between neighbouring centres. In particular, centres with a small growth rate (small CGF) interfere with the neighbouring centres after a longer time than those with a higher growth rate (high CGF).

The PVT method is the simplest case of constant-rate growth. Therefore, the cell size distribution of a PVT reflects exactly the distribution of the half distances of the neighbouring centres. In a sample created by the PVT method, the cell radius computed from the cell volume and from the mean PIs distance show exactly the same distribution and almost the same values. A change in the size distribution is strictly connected to any change of the arrangement of the centres. For instance, the CVT method drives the centres towards a configuration where the distribution of plane interface distances is comparable with the target cell volume distribution. As previously noted, this leads to non spherical cells; in particular, cells with the largest standard deviation are more anisotropic [41]. Removing the constraints imposed by the Voronoi construction, allows moving the centres independently of the cell shape: a full control over anisotropy (and therefore roundness of the cells) is thus possible.

Figure 9 shows a clear parabolic relationship between σ of the CGF (σ_{in}) and both μ and σ of the corresponding cell volume distribution. Independent of the number of centres, the two parabolas can be parameterised as $\mu = -0.0674 - 2.0149\,\sigma_{\text{in}}^2$ and $\sigma = 0.4454 + 2.2455\,\sigma_{\text{in}}^2$.

The result is compatible with the PVT where $\sigma = 0.445$ is obtained when fitting the resulting distribution with a lognormal [26]. The data spread around the best fit in Figure 9 can be related to the statistics of the corresponding distributions. The picture does not change if the size of the box, the number of centres and the μ of the lognormal CGF distribution are changed.

Systematic effects related to the simulation parameters can be detected also for other topological properties such as the average cell surface density (CSD), i.e. the ratio between the cumulative cell surface and the box volume. Figure 10 shows the trend of the CSD versus the σ of the input distribution of CGF.

The average cell surface density decreases with increasing distribution width. The trend is similar independently of the number of centres, but the actual values steadily increase with the increasing quantity of generators. An increase of the standard deviations of CGF distribution causes a general decrease of the global surface of the cells: in fact, the larger the spread of the cell sizes, the smaller the volumetric contribution of smaller cells for a constant box volume. It is well know that in a box of constant volume a system of smaller spheres would have a larger surface than a system of large ones. For a given distribution, moreover, an increase in the number of centres causes a decrease of the mean cell size, and therefore a corresponding increase in the cell surface density, as experimentally observed.

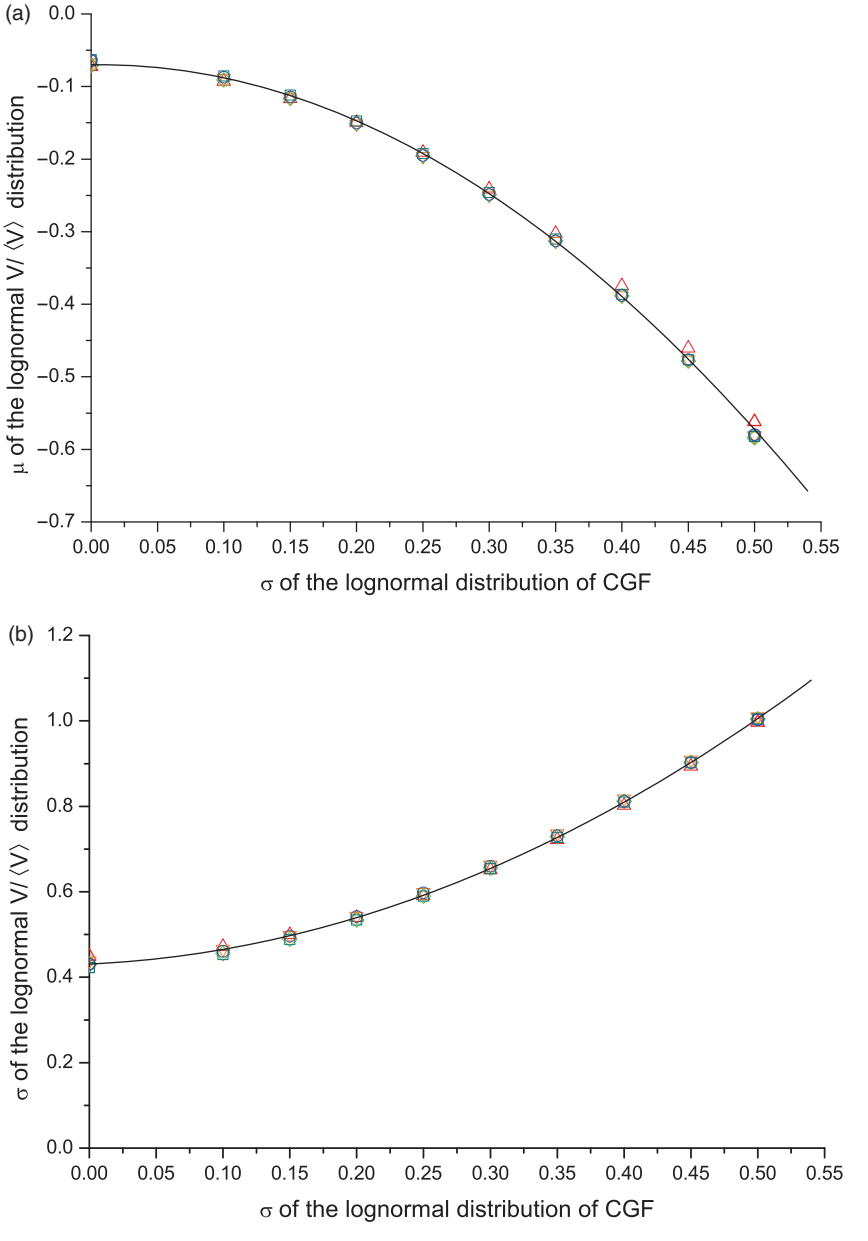

Figure 9. Relationship between the σ of the input lognormal distribution of CGF and the parameters μ and σ ((a) and (b), respectively) of the resulting best fitted lognormal output distribution of $V/\langle V\rangle$ for specimens of increasing number of centres (1000: up triangle, 2000: down triangle, 3000: diamond, 4000: square, 5000: circle).

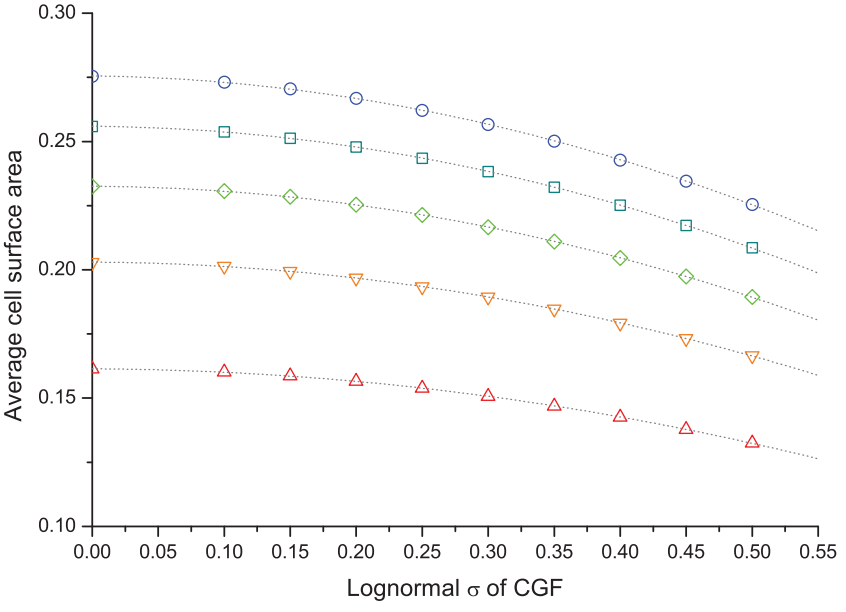

Figure 10. Dependence of the cell surface density versus the σ of the input CGF for an increasing number of centres (1000: up triangle, 2000: down triangle, 3000: diamond, 4000: square, 5000: circle).

3.4. *Computing performance*

We have shown that the MVT can directly provide a microstructure with a given size distribution variance and with a shape close to lognormal. Unlike the VT, however, computing time for the MVT is not linearly related to the number of centres, but it depends on the actual properties of the input distribution. This is a consequence of simultaneously dealing with all centres and corresponding growth factors to compute the shape of the resulting cell, while keeping full record of the voids.

The increase in computing time is clear in Figure 11, which shows the total time required to build a model of 1000 grains in a box with PBCs when increasing the σ of the CGF distribution. Calculations were performed on an Intel Core 2 processor (4 physical cores) at 2.8 GHz in multithread mode (4 computing threads). Clearly the MVT needs a longer time to deal with the cases where a centre is surrounded by other centres having a wide variety of CGF: a broader CGF distribution increases the probability of this condition to be met. Of course, as previously pointed out, the broader the distribution, the larger the fraction of void space (cf. Figure 5b), thus the longer time and memory for bookkeeping of information about intersection of interface planes.

When compared with the few available literature data on advanced tessellation methods (cf. [49]), the actual values in Figure 11 suggest that MVT can be orders of magnitude faster than the available algorithms to obtain a target distribution of cells. In fact, to obtain a target lognormal distribution of 1000 grains on a computer with 80 cores, Suzudo and Kaburaki [49] needed at least 1150 seconds of CPU time

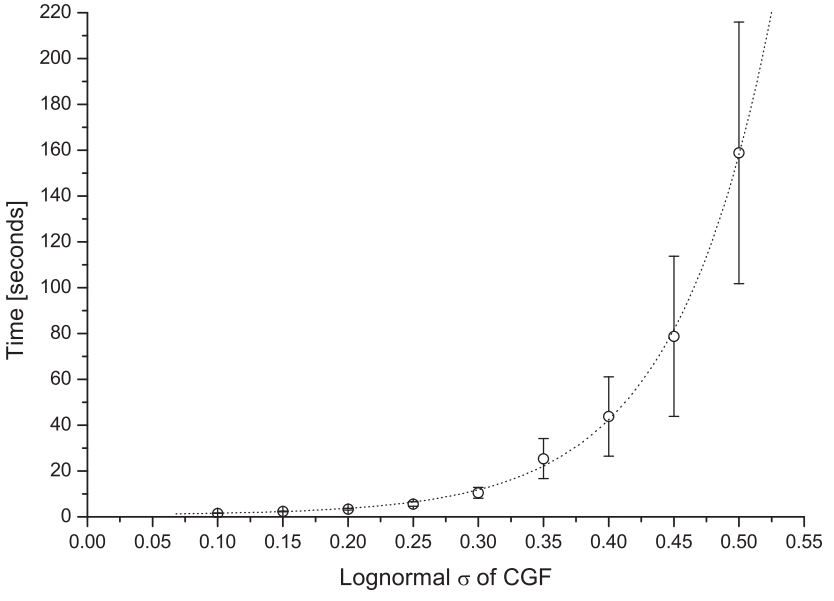

Figure 11. Time required by the MVT method to compute the microstructure (i.e. to identify the faces of all cells) for the MVT 1000 set of specimens.

(the actual value might be higher depending on the target precision). Scaled to a 4-cores machine such as the one employed here, this would correspond to more than 23,000 s, clearly out of range with respect to Figure 11. No data are available for the CVT proposed in [41]: however, the authors state that at least 500 steps are needed to reach a good level of convergence, versus a single step required by MVT.

4. Conclusion

A modified Voronoi tessellation (MVT) has been proposed to simulate a realistic microstructure. To obtain that, MVT starts with a random distribution of centres in a box (with or without periodic boundary conditions) and builds the corresponding cells by relaxing the Voronoi constraints on the cell–cell interfaces, i.e. by shifting and rotating them with respect to the midpoint between neighbouring centres. The resulting microstructure (pattern) is characterised by the presence of voids that can be easily eliminated when filling the cells with atoms. A one-to-one relationship between the input model parameters and the characteristics of the output distribution has been found, allowing a target distribution to be directly obtained. For instance, a lognormal distribution of grain sizes can be directly simulated with a 5% level of significance. Computing time increases with the target distribution width, but it is highly competitive to literature alternatives providing similar results.

Acknowledgements

The authors wish to thank Prof. Mo Li (Georgia Institute of Technology) for helpful discussions.

References

[1] H. Gleiter, Acta Mater. 48 (2000) p.1.
[2] C. Suryanarayana and C.C. Koch, Hyperfine Interact. 130 (2000) p.5.
[3] S. Mahadevan and Y. Zhao, Comput. Meth. Appl. Mech. Eng. 191 (2002) p.3651.
[4] G.P. Zheng, D. Gross and M. Li, Phys.: Stat. Mech. Appl. 355 (2005) p.355.
[5] B. Zhu, R.J. Asaro, P. Krysl, K. Zhang and J.R. Weertman, Acta Mater. 54 (2006) p.3307.
[6] M.F. Vaz and M.A. Fortes, Scripta Metall. 22 (1988) p.35.
[7] K.J. Kurzydlowski, Scripta Metall. Mater. 24 (1990) p.879.
[8] D. Gross and M. Li, Appl. Phys. Lett. 80 (2002) p.746.
[9] Y. Liu, J. Zhou and X. Ling, Mater. Sci. Eng. A 527 (2010) p.1719.
[10] E.S. Fedorov, ACA Monograph No.7 (1971) p.50.
[11] A.L. Mackay, Phys.: Stat. Mech. Appl. 114 (1982) p.609.
[12] R. Penrose, Bull. Inst. Math. Appl. 10 (1974) p.266.
[13] K.N. Ishihara and P.H. Shingu, J. Phys. Soc. Jpn 55 (1986) p.1795.
[14] B. Delaunay, Math. Nat. Sci. Div. 6 (1934) p.793.
[15] L. Muche, J. Stat. Phys. 84 (1996) p.147.
[16] R. Sibson, Scand. J. Stat. 7 (1980) p.14.
[17] F. Aurenhammer, ACM Comput. Surv. 23 (1991) p.345.
[18] S. Kumar, S.K. Kurtz, J.R. Banavar and M.G. Sharma, J. Stat. Phys. 67 (1992) p.523.
[19] V. Lucarini, J. Stat. Phys. 134 (2009) p.185.
[20] V. Lucarini, J. Stat. Phys. 130 (2008) p.1047.
[21] N.W. Thomas, Acta Crystallogr. B 52 (1996) p.939.
[22] X. Xue, F. Righetti, H. Telley, T.M. Liebling and A. Mocellin, Phil. Mag. B 75 (1997) p.567.
[23] C. Lautensack and S. Zuyev, Adv. Appl. Probab. 40 (2008) p.630.
[24] J. Farjas and P. Roura, Phys. Rev. B 78 (2008) 144101.
[25] J. Møller, Adv. Appl. Probab. 24 (1992) p.814.
[26] J.L. Meijering, Philips Res. Rep. 8 (1953) p.270.
[27] F. Baccelli and B. Błaszczyszyn, Adv. Appl. Probab. 33 (2001) p.293.
[28] E.N. Gilbert, Ann. Math. Stat. 33 (1962) p.958.
[29] R. Van de Weygaert, Astron. Astrophys. 283 (1994) p.361.
[30] M. Tanemura, J. Microsc. 151 (1988) p.247.
[31] F. Járai-Szabó and Z. Néda, Phys.: Stat. Mech. Appl. 385 (2007) p.518.
[32] A.L. Hinde and R.E. Miles, J. Stat. Comput. Simulat. 10 (1980) p.205.
[33] A. Goldman, Ann. Appl. Probab. 20 (2010) p.90.
[34] P. Calka, Adv. Appl. Probab. 35 (2003) p.551.
[35] A. Goldman and P. Calka, Ann. Inst. H. Poincaré Probab. Stat. 39 (2003) p.1057.
[36] R.E. Miles and R.J. Maillardet, J. Appl. Probab. A 19 (1982) p.97.
[37] J. Møller, *Lectures on Random Voronoi Tesselations*, Springer-Verlag, New York, 1994.
[38] J.M. Drouffe and C. Itzykson, Nucl. Phys. B 235 (1984) p.45.
[39] N.H. Christ, R. Friedberg and T.D. Lee, Nucl. Phys. B 202 (1982) p.89.
[40] H.J. Hilhorst, J. Stat. Mech. (2005) P09005. DOI: 10.1088/1742-5468/2005/09/P09005.
[41] T. Xu and M. Li, Phil. Mag. 89 (2009) p.349.
[42] F.N. Rhines and B.R. Patterson, Metall. Trans. A 13 (1982) p.985.
[43] C. Wang, G. Liu, G. Wang and W. Xue, Mater. Sci. Eng A 454–455 (2007) p.547.
[44] D. Dierickx, B. Basu, J. Vleugels and O. Van der Biest, Mater. Char. 45 (2000) p.61.
[45] Y. Takayama, N. Furushiro, T. Tozawa, H. Kato and S. Hori, Mater. Trans. JIM 32 (1991) p.214.
[46] R.Y. Yang, R.P. Zou and A.B. Yu, Phys. Rev. E 65 (2002) 041302.

[47] Z. Fan, Y. Wu, X. Zhao and Y. Lu, Comput. Mater. Sci. 29 (2004) p.301.
[48] Y. Wu, W. Zhou, B. Wang and F. Yang, Comput. Mater. Sci. 47 (2010) p.951.
[49] T. Suzudo and H. Kaburaki, Phys. Lett. A 373 (2009) p.4484.
[50] A. Leonardi, P. Scardi and M. Leoni, Appl. Phys. Lett. (under review).
[51] T. Xu and M. Li, Phil. Mag. 90 (2010) p.2191.
[52] H. van Swygenhoven, Science 296 (2002) p.66.
[53] H.J. Hilhorst, J. Stat. Mech. (2009) P08003. DOI: 10.1088/1742-5468/2009/08/P08003.
[54] M. Tanemura, Forma 18 (2003) p.221.
[55] F.T. Lewis, Anat. Rec. 38 (1928) p.341.
[56] D.A. Aboav and T.G. Langdon, Metallography 1 (1969) p.333.
[57] P.A. Beck, Adv. Phys. 3 (1954) p.245.
[58] N. Rivier, Phil. Mag. B 52 (1985) p.795.
[59] S.N. Chiu, Mater. Char. 34 (1995) p.149.